PHYSICAL REVIEW B VOLUME 47, NUMBER 15 15 APRIL 1993-I

Structure and band bending at Si/GaAs(001)-(2×4) interfaces

S. A. Chambers* and V. A. Loebs
Boeing High Technology Center, Seattle, Washington 98124-2499
(Received 1 May 1992; revised manuscript received 4 January 1993)

We have grown thin, epitaxial overlayers of undoped and As-doped Si on As-stabilized *n*- and *p*-type GaAs(001)-(2×4) in order to investigate the influence such overlayers have on band bending in the surface depletion region. We have carried out structural, chemical, and electronic investigations of the resulting interfaces by means of x-ray photoemission spectroscopy, low-energy electron diffraction, and x-ray photoelectron diffraction. Strained, epitaxial overlayers of Si could be grown for thicknesses of up to 10 ± 1 Å at a growth temperature of 400 °C. The perpendicular lattice constant of the overlayer is estimated to be 5.32 ± 0.10 Å in this coverage regime. An interface reaction between Si and Ga is observed for all coverages. Growth of undoped Si overlayers essentially conserves the band bending that exists on the free surface ($\sim$0.6 eV on *n*-type GaAs and $\sim$0.5 eV on *p*-type GaAs). However, the growth of heavily As-doped Si flattens the bands to $\sim$0.3 eV on *n*-type GaAs, but increases the band bending on *p*-type GaAs to $\sim$0.8 eV. The influences that undoped and n^+-doped Si overlayers have on the surface band bending are readily explained by a simple model in which it is recognized that (1) epitaxial Si does not unpin the Fermi level in the sense that interface states are eliminated, and (2) a decrease (increase) in the net electric field in the depletion region of *n*-type (*p*-type) GaAs is brought about by charge transfer from the n^+-doped Si epilayer to the near-surface region of the GaAs substrate.

I. INTRODUCTION

The fixed band bending exhibited by both free surfaces and interfaces of GaAs(001) places definite limitations on the utility of this semiconductor in device and circuit technology.[1] The tendency of the surface Fermi level to pin near the midgap position at interfaces to virtually all metals precludes the possibility of forming a true Ohmic contact. Device technologists must resort to a rather crude process involving extensive alloying of a multicomponent metalization at the interface, with the concomitant indiffusion of one of the components of the metal mix acting to heavily dope the GaAs.[2] This high degree of doping results in a very narrow depletion region, through which conduction-band electrons must tunnel, giving rise to what is in effect a rectifying contact that is dominated by tunneling. Such a contact is essentially "pseudo-Ohmic." Also, the inability to form rectifying contacts with very high Schottky-barrier heights by conventional metalizations prevents the fabrication of gate structures with negligible leakage current.

Both of these problems can be avoided by finding ways to gain control of band bending on the GaAs side of the interface. A few techniques have been reported in the literature that appear to enable such control. One of the more promising techniques centers around the use of doped interlayers of a group-IV semiconductor (either Si or Ge). It has been found that the growth of an *n*-type Ge or *n*-type Si (*p*-type Ge or *p*-type Si) interlayer between *n*-type GaAs(001) and a metal deposit results in movement of the Fermi level much closer to the conduction (valence) band than occurs in the absence of the interlayer.[3–7] In addition, it has been reported that the use of a thin Si interlayer between GaAs and AlAs allows some degree of control of the heterojunction band offset.[8] Furthermore, enhanced performance in metal-insulator-semiconductor (MIS) structures has evidently resulted from the use of a thin Si interlayer between the insulator and the III-V semiconductor.[9–13] It has been suggested that these improvements result because the Si interlayer gives rise to an unpinned Fermi level on the GaAs side of the interface, although a recent photoemission study of ultrathin, undoped Si epilayers on very heavily doped *n*- and *p*-type GaAs(001) appears to refute this possibility.[14] A recent modeling study suggests that charge compensation of the *n*-type GaAs depletion region by carriers from a highly doped Si overlayer is what gives rise to the range of observed Fermi-level motion.[15]

In this paper, we describe a detailed investigation of the interfaces formed between undoped and n^+-doped Si and moderately doped *n*- and *p*-type GaAs. Our goals were (1) to further investigate the question of whether or not the Fermi level is unpinned at the Si/GaAs interface and (2) to determine the mechanism by which a substantial range of Fermi-level motion is achieved when the Si overlayer is heavily doped *n* type. We conclude that the Fermi level is, in fact, pinned at the Si/GaAs interface, in agreement with a recent study involving GaAs that was much more heavily doped.[14] Our results demonstrate that the Fermi level remains pinned at nearly the same position as that found on the free GaAs surface. In addition, we present evidence that the reduction (increase) in band bending brought about by growth of n^+-doped Si on *n*-type GaAs (*p*-type GaAs) is the result of charge compensation of the depletion layer by carriers from the Si overlayer.

 ©1993 The American Physical Society

II. EXPERIMENTAL

All Si growths were performed on As-capped, molecular-beam-epitaxy (MBE) grown *n*- or *p*-type GaAs buffer layers, which were in turn grown on semi-insulating GaAs substrates in a Varian Generation II MBE system. The dopants were Si and Be for the *n*- and *p*-type buffer layers, respectively, and the doping density was $\sim 5\times 10^{17}$ cm^{-3}. The As cap was desorbed by heating for several minutes at $\sim$450 °C after transfer of the wafers from the Varian MBE system to a smaller MBE chamber appended to a surface analytical chamber. The resulting GaAs surfaces were As stabilized, and exhibited either a $(2\times 4)/c(2\times 8)$ or a (1×6) low-energy electron diffraction (LEED) pattern. A slight reduction in As 3*d* intensity was detected in going from the former to the latter LEED pattern, in keeping with previous characterization of these surfaces.[16]

MBE growth of Si from a Knudsen cell with a tungsten crucible was carried out under ultrahigh vacuum conditions, or in an As_4 overpressure in the low to mid 10^{-9} torr range. Si overlayer thickness was measured with a quartz-crystal oscillator (QCO), and an absolute thickness calibration was carried out by obtaining Rutherford-backscattering (RBS) measurements of the total backscattering yield in a random direction for the thicker overlayers.

After transfer under UHV conditions from the growth chamber to the analytical chamber, high-energy resolution x-ray photoelectron spectra (XPS) were obtained at normal emission using a Surface Science Instruments Series 300 photoelectron spectrometer that is equipped with a monochromatic Al $K\alpha$ x-ray source, a hemispherical energy analyzer, and a multichannel detector. All high-resolution spectra were obtained with an x-ray beam diameter of 300 μm and a pass energy of 25 eV. The total resolution, as judged by the full width at half maximum (FWHM) of the Au $4f_{7/2}$ peak from clean, polycrystalline Au, is $\sim$0.73 eV. For these settings, the Au $4f_{7/2}$ peak was also used to regularly calibrate the spectrometer electronics so that absolute core-level binding energies could be determined with an accuracy of $\pm$0.02 eV. This procedure allows the determination of band bending within the GaAs depletion region with an accuracy of $\pm$0.04 eV.

This spectrometer is readily converted from an angle-integrating mode to an angle-resolved mode by externally accuating one of two apertures at the spectrometer lens entrance. Scanned-angle x-ray photoelectron diffraction (XPD) measurements were then made by rotating the specimen about one of two axes (polar or azimuth) while keeping the other constant.[17] In this way, angular distributions could be obtained with an angular resolution and an absolute angular precision of $\pm$3.3° and $\pm$0.2°, respectively, in either the polar or azimuthal angle.

Surface topography of the epitaxial films was monitored by means of atomic-force microscopy (AFM). Samples were removed from the UHV system and inserted into a TopoMetrix (TMX) 200 AFM in order to obtain high-resolution images of the surface.

III. RESULTS AND DISCUSSIONS

A. Structural characterization by LEED and XPD and absolute coverage calibration

Si epilayer growth occurs in a laminar fashion at a growth temperature of 400–500 °C for coverages up to several monolayers (ML), as judged by two separate experimental probes. First, Bratina *et al.* report a transition from a streaky to a spotty reflection high-energy electron diffraction (RHEED) pattern at coverages of 4–8 ML, indicating a transition from laminar to island growth.[18] Second, in the present investigation, overlayers grown with a thickness of $\sim$4 ML exhibit a Si 2*p* zeroth-order, forward-scattering photoelectron diffraction peak near $\theta=45°$ in the (010) azimuthal plane, but do not exhibit any such peak along the surface normal. These directions coincide with the [101] and [001] low-index directions, respectively. Assuming completely laminar growth, such peaks should appear at $\theta=\sim 45°$ and 90° as a result of third- and fifth-layer formation, respectively. Atoms in the third (fifth) layer act as forward scatterers for photoelectrons generated in the first layer when the Si 2*p* intensity is measured at $\theta=45°$ (90°), giving rise to intensity maxima.[19] The absence of a peak along the surface normal for a deposit of $\sim$4 monolayer equivalents indicates that the growth is essentially laminar, in agreement with previous RHEED results.[18]

The transition from laminar growth to three-dimensional island growth is detected in the present work by comparing the overlayer thickness as judged by the RBS-calibrated QCO with the apparent thickness derived from the rate of attenuation of Ga 3*d* core-level intensity. With laminar growth, and in the absence of Ga outdifussion, the Ga 3*d* intensity is expected to drop exponentially with coverage. The Ga 3*d* reduced intensity α (defined as $\ln[I(d)/I(0)]$) can be related to the overlayer thickness d by the simple relationship $d=-\alpha\lambda\sin\theta$, where λ is the electron attenuation length and θ is the emission angle relative to the surface plane. We have used a value of 24$\pm$2 Å for λ, as taken from calculations by Tanuma *et al.* for 1450 eV electrons propagating through bulk Si.[20] We show in Fig. 1(a) the plot of the total amount of Si deposited, as judged by the QCO, against the apparent overlayer thickness, as determined by the method outlined above. The error estimates were assigned as follows. Based on the high degree of stability in our x-ray flux and the excellent signal-to-background ratio in the Ga 3*d* peak, we assume that the absolute error in the Ga 3*d* peak intensity is negligible compared to the uncertainty in λ. Therefore, the latter dominates the total error in d (the abcissa in Fig. 1).

The error assigned to the total amount of Si deposited is based on an independent calibration by RBS. The total amount of Si in an overlayer that was estimated to be $\sim$80 Å thick by the QCO was determined to be $(4.5\pm 0.8)\times 10^{16}$atoms/cm^2 by RBS. XPD results for this coverage indicate that the film was completely relaxed, as discussed below. Thus, using the surface atom density for bulk Si (6.8×10^{14} cm^{-2}), this coverage is equivalent to 66$\pm$12 ML, or 90$\pm$16 Å. Assigning an uncertainty of $\pm$10 Å ($\pm$12%) to our QCO reading brings

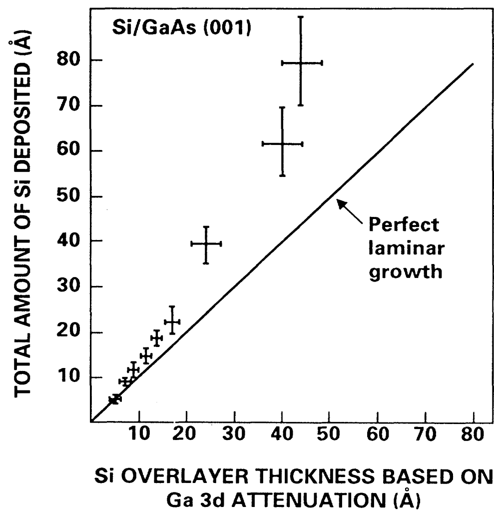

FIG. 1. Total Si deposit, as judged by a QCO that was calibrated by Rutherford backscattering, plotted against Si overlayer thickness as determined by the attenuation of the Ga 3*d* photoelectron peak intensity. Perfectly laminar growth would result in a slope of unity. The deviation from unity is consistent with island formation, which was directly observed by AFM.

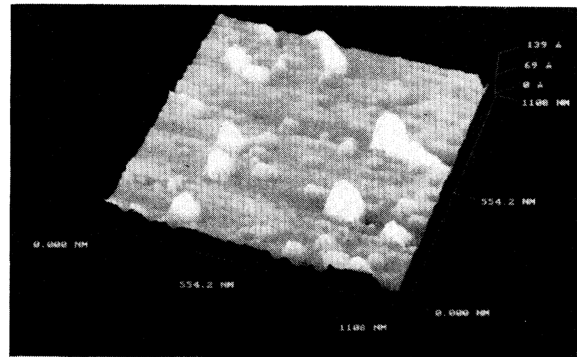

FIG. 2. AFM image of a 60-Å Si deposit, as judged by the QCO. The film thickness based on Ga 3*d* attenuation was 34 Å. The tendency of Si to form islands on GaAs is the result of its higher surface-free energy. The presence of islands explains the discrepancy between the QCO film thickness and the thickness based on Ga 3*d* attenuation.

the QCO and RBS coverages into agreement within experimental error. We have therefore assumed an error of $\sim\pm12\%$ for all QCO coverage determinations.

The Si overlayer thickness based on Ga 3*d* attenuation is consistently less than the Si deposit thickness, and the difference increases with increasing coverage. This result suggests that either three-dimensional island formation or Ga outdiffusion occurs. There is clearly an interface reaction between Ga and Si, as judged by the presence of an additional spin-orbit doublet in the high-resolution Ga 3*d* spectra, which are discussed in Sec. III B. However, extensive outdiffusion can be ruled out because the fraction of the total Ga 3*d* intensity corresponding to interface reaction product does not increase with coverage in a way expected for a surface-segregated species. If surface segregation of the disrupted Ga species occurs, the fraction of the total intensity corresponding to this species should increase monotonically with coverage, and such an increase is not observed. The component of the peak originating in the substrate should be completely attenuated by coverages in excess of $\sim 3\lambda$ (75 Å). However, a measurable Ga 3*d* spectrum from the substrate persists for deposits up to 80 Å. Therefore, the persistence of Ga 3*d* substrate emission is best interpreted in terms of island growth. In this case, the core-level attenuation gives an *average* thickness over the dimensions of the x-ray irradiation area (diameter 800 μm for these measurements). If the height of the islands exceeds the escape depth of the photoelectrons, there will be no signal from the substrate beneath the islands. More laminar regions between islands will be thinner than what is expected on the basis of the QCO thickness, and the apparent film thickness based Ga 3*d* attenuation will be less than the QCO reading.

In order to verify that island formation does indeed occur, we obtained AFM images for an epitaxial film that was 60 Å thick as judged by the QCO, and 34 Å based on Ga 3*d* attenuation. One of these micrographs is shown in Fig. 2. Island formation is clearly visible. The larger islands to the right are ~100 Å tall and ~1300 Å wide. The islands of intermediate size to the left are ~40 Å tall and ~1000 Å at the base. The tendency of Si to form is-

5Å (3 ML) (2x1)-Si/n-GaAs(OO1)

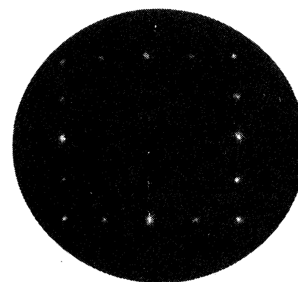

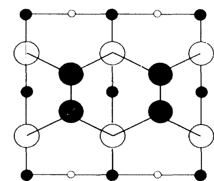

LEED - 48 eV

Substrate orientation

- ● -Surface As
- ○ -Second-layer Ga
- • -Third-layer As
- ∘ -Fourth-layer Ga

FIG. 3. Orthogonal (2×1) (LEED) patterns for a 5-Å epitaxial overlayer of Si on GaAs(001), grown at 400 °C. At the right is a structural diagram of the substrate showing the substrate crystal orientation relative to the overlayer LEED pattern.

lands on GaAs is a result of its high surface free energy. The presence of these islands on the surface explains the discrepancy between the thickness as determined by the QCO and Ga 3*d* attenuation.

We show in Fig. 3 a typical LEED pattern for strained, epitaxial, undoped Si on GaAs(001) when grown to a total coverage of less than or equal to ~10 Å. Also shown on the right-hand side is the substrate orientation prior to growth of the Si overlayer. This particular growth was carried out on a substrate that exhibited a (1×6) LEED pattern, although the same pattern appears after growth on (2×4)/*c*(2×8) substrate surfaces. The pattern reveals orthogonal (2×1) domains, as evidenced by the extra spots along both horizontal and vertical rows. This pattern has also been observed in previous investigations over a range of coverages.[18,21,22] The double periodicity is undoubtedly due to Si dimers in the surface layer, although the detailed surface and interface structure that gives rise to orthogonal (2×1) domains is not known at this time.

Si overlayers produced by coevaporation with As_4 showed a very weak (1×1) LEED pattern or, more frequently, no LEED pattern at all. The absence of a LEED pattern after the growth of doped Si overlayers is ascribed to the buildup of excess, disordered arsenic on the surface, which was detected by angle-integrated XPS. Arsenic condensation on the surface probably occurred during postgrowth cooldown; the residence time of As_4 in the chamber, as judged by a residual gas analyzer, exceeds the time required for the sample to cool to below the desorption temperature of As_4. XPD angular distributions of Si 2*p* intensity showed that Si epilayers of the same thickness with and without As doping possessed the same overall structural quality, establishing that the lack of a LEED pattern for doped specimens was indeed due to the presence of excess As on the surface, rather than disorder in the epilayer. XPD scans of As 3*d* intensity from doped Si overlayers of sufficient thickness to completely attenuate Ga 3*d* emission from the substrate at shallow polar angles were featureless, indicating that the surface As was present in disordered form. As atoms incorporated at lattice sites in the Si layer would exhibit intensity modulations characteristic of the diamond lattice, as has been observed for P in epitaxial Ge on GaAs(001).[7] However, such modulations would be washed out by the constant intensity from disordered arsenic on the surface, particularly if the amount of arsenic in the surface phase exceeds that in the Si lattice.

In Fig. 4 we show Si 2*p*, Ga 3*d*, and As 3*d* photoelectron azimuthal angular distributions at a polar angle of 35° obtained for such a thin As-doped Si overlayer. This scan passes through the ⟨111⟩ family of directions that contains bonds between atoms in adjacent layers with the nearest-neighbor distance in either the diamond or zingblende structure. Strong forward scattering occurs along these directions, giving rise to peaks at $\phi=0°$, 90°, and 180° in the overlayer, at $\phi=90°$ in the Ga 3*d* scan, and at $\phi=0°$ and 180° in the As 3*d* scan.[17] The diffraction modulations observed in the Ga and As 3*d* scans are out of phase with one another by 90°, in keeping with the structural differences between the cation and anion sublattices.

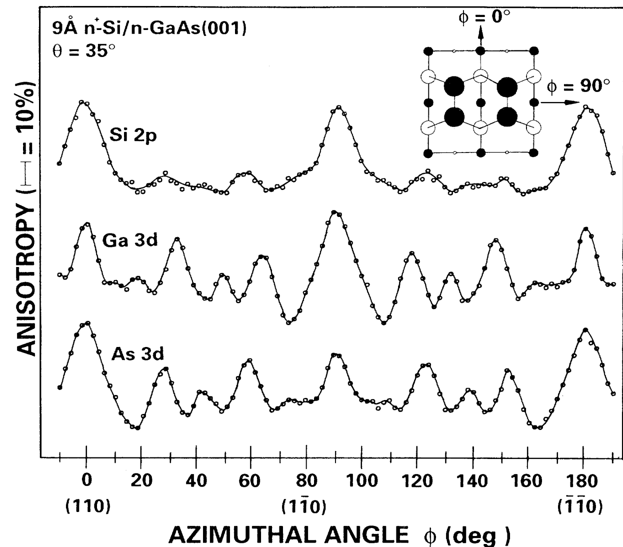

FIG. 4. XPD azimuthal scans of Si 2*p*, Ga 3*d*, and As 3*d* intensities for a 9-Å As-doped Si overlayer on *n*-type GaAs(001). The detailed peak and valley structure seen in the three scans establishes that the interface is abrupt (see text).

The Si 2*p* scan shows the same structure as that measured for bulk Si(001)-(2×1), demonstrating that the majority of Si atoms in the deposit have formed a diamond lattice in the epilayer, as opposed to indiffusing and occupying substitutional sites in the substrate zinc-blende crystal.[23] In addition, averaging the Ga 3*d* and As 3*d* scans produces an angular distribution that is extremely close in appearance to that associated with Si 2*p* photoemission. This outcome is precisely what is expected given the fact that photoemission is an incoherent process. There is no unique phase relationship between photoelectron waves emitted from different lattice sites. Therefore, the net photoelectron diffraction pattern emitted from a given lattice is the incoherent sum of intensities from all emitting lattice sites. The diamond lattice becomes equivalent to the zinc-blende lattice if the cationic and anionic species in the latter are reduced to a single species. Thus, the overall photoelectron diffraction pattern from a diamond structure should, in fact, be the same as the sum of diffraction patterns from the two atomic species in a binary zinc-blende structure.

In order to determine the critical thickness of and tetragonal distortion in epitaxial films of Si on GaAs(001), we have measured polar scans of Si 2*p* intensity in the (010) azimuthal plane. These scans exhibit strong zeroth-order forward-scattering peaks at polar angles near 45° and 90°, corresponding to the [101] and [001] low-index directions, respectively. In addition, higher-order interference structure is also seen at $\theta\sim70°$. The peak along [101] associated with the Si epilayer scan is shifted to lower polar angle relative to 45.0°, the angle expected and observed for unstrained Si(001). This shift is the result of tetragonal distortion associated with the 4% lattice mismatch between Si ($a=5.43$ Å) and

GaAs(001) ($a = 5.65$ Å). Precise measurement of the angle at which this peak occurs, which we designate as $\theta_{[101]}$, provides an estimate of the perpendicular lattice constant in the epifilm $a_\perp$.[19] This determination can be made only if the in-plane lattice constant, $a_\parallel$ is known. The relationship between $a_\perp$, $a_\parallel$ and $\theta_{[101]}$ is $a_\perp = a_\parallel \tan\theta_{[101]}$.

We plot in Fig. 5 the angle $\theta_{[101]}$ vs Si over layer thickness, as determined from the attenuation of the Ga 3d substrate intensity. A constant value of $43.3 \pm 0.3°$ is observed for thicknesses up to ~10 Å, above which film relaxation begins to occur. Film relaxation is detected by a gradual increase in $\theta_{[101]}$. The film is essentially completely relaxed by a thickness of 40 Å, as evidenced by the fact that $\theta_{[101]}$ reaches a value of $44.9 \pm 0.2°$ by this coverage. The LEED pattern remains a sharp orthogonal (2×1) for coverages up to ~10 Å, above which the spots begin to broaden. There was no detectable change in the position of the (10) LEED beam relative to the (00) beam in going from the clean surface to thin Si epilayers of thickness less than or equal to 10 Å. Therefore, we conclude that the in-plane lattice constant remains equal to that of the substrate for coverages up to 10 Å. The increase in both $\theta_{[101]}$ and the width of the (10) and (00) LEED beams for coverages above 10 Å suggests that the critical thickness is 10 ± 1 Å. This overlayer thickness based on Ga 3d attenuation corresponds to a total deposit of ~13 Å as judged by the QCO. This value is in excellent agreement with results by Zalm, Maree, and Olthof for Si on GaAs(001)$-c(8\times2)$ at ~600 °C.[22] These authors noted a change in spacing between the RHEED diffraction spots at a coverage of 10 ML, which is equivalent to ~13 Å. Using $a_\parallel = 5.65$ Å and $\theta_{[101]} = 43.3°$ for thicknesses below ~10 Å, we estimate $a_\perp$ to be equal to 5.32 ± 0.10 Å below the critical thickness.

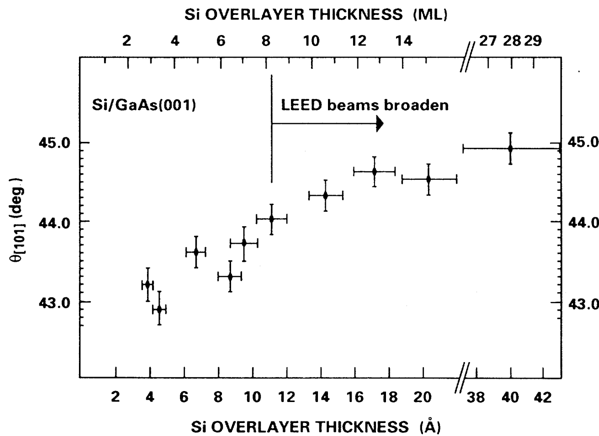

FIG. 5. Polar angle at which the Si 2p zeroth-order forward-scattering peak appears along [101] in scans through the (010) azimuthal plane as a function of Si coverage. Deviations from 45.0° indicate tetragonal distortion associated with lattice mismatch. $\theta_{[101]}$ remains constant at $43.3 \pm 0.2°$ for coverages up to 10 ± 1 Å, above which $\theta_{[101]}$ steadily increases as lattice relaxation occurs.

B. Chemistry of interface formation and band bending by XPS

We have obtained high-resolution XPS spectra for undoped and n^+-doped Si overlayers on n- and p-type GaAs(001) for coverages above and below the critical thickness. Our goals were (1) to learn something about the chemistry associated with interface formation, (2) to determine whether or not the Fermi level is pinned as a result of coherent bonding across the IV/III-V interface and to see if the nucleation of misfit dislocations affects the Fermi-level position, and (3) to elucidate the mechanism responsible for the substantial extent of Fermi-level movement brought about by changing the doping in the Si overlayer. Accordingly, we have measured or derived from experimental measurements several relevant quantities, which are shown on the energy diagrams found in Fig. 6. These include $E_{\mathrm{Ga}3d}$ and $E_{\mathrm{Si}2p}$, the absolute Ga 3d and Si 2p core-level binding energies before and after heterojunction formation relative to the Fermi level; ΔE_{CB}, the conduction-band offset; $\Delta E_{\mathrm{CB\text{-}FL}}$, the energy difference between the conduction-band minimum and the Fermi level on the GaAs side of heterojunctions formed with n-type GaAs; and $\Delta E_{\mathrm{FL\text{-}VB}}$, the splitting between the Fermi level and the valence-band maximum for heterojunctions formed with p-type GaAs. In addition, we have extracted from $\Delta E_{\mathrm{CB\text{-}FL}}$ the electronic state density in the forbidden gap (n_s) for both the free surface of GaAs(001) and Si/GaAs(001) heterojunctions.

The valence-band offset for a strained-layer heterojunction can, in principle, be derived from core-level and valence-band binding energies from the relation[24,25]

$$\Delta E_{\mathrm{VB}} = [(E^A_{\mathrm{CL}} - E^A_{\mathrm{VB}}) + \delta_s] - (E^B_{\mathrm{CL}} - E^B_{\mathrm{VB}}) - \Delta E_{\mathrm{CL}} . \quad (1)$$

Here, ΔE_{CL} is the binding-energy difference between representative core levels at the A/B heterointerface, E_{CL}-E_{VB} is the energy difference between the representative core level and the valence-band maximum for clean, *unstrained* surfaces of semiconductors A and B, and δ_s

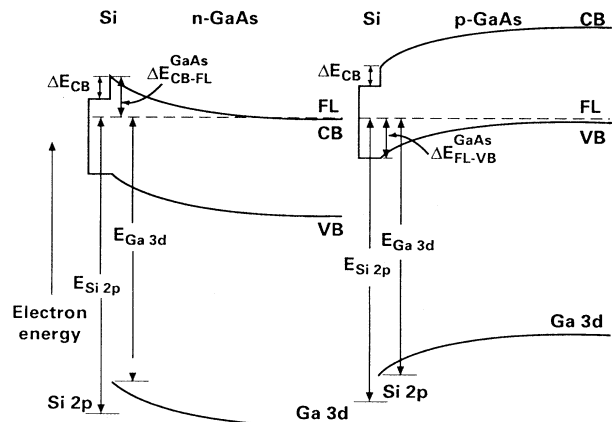

FIG. 6. Energy diagram illustrating the quantities extracted from analysis of core-level photoemission spectra for interfaces of Si with n- and p-type GaAs(001).

represents the change in energy of the valence-band maximum in semiconductor A brought about by the biaxial (in-plane) strain associated with lattice mismatch. Such strain is believed to produce a splitting in the light-hole, heavy-hole, and spin-orbit bands, resulting in changes in the total valence-band spectrum that modify the energy of the valence-band maximum. The principal difficulty associated with using this technique is in finding a reliable value for δ_s. Yu *et al.* have attempted to determine an analytic expression for δ_s as a function of strain for Si by carrying out an elaborate set of experiments in which strained Si overlayers were grown on thick, fully relaxed Ge_xSi_{1-x} films, which were in turn grown on Ge(001).[26] The Ge mole fraction was varied from 0 to 3.0. The Si overlayer thickness was sufficient to completely attenuate valence-band emission from the alloy, yet small enough that the critical thickness was not exceeded. Therefore, the Si overlayer was subjected to a maximum biaxial strain equivalent to a 0.07-Å deviation in the in-plane lattice constant from the bulk Si value. The resulting expression for the strain correction is $\delta_s = 1.96\,(a_{\parallel} - 5.431)$ (eV). We have used this expression in conjunction with Eq.(1) to attempt a determination of $\Delta E_{\rm VB}$.

In addition, we have used Ga $3d$ core-level binding energies to determine the energy difference between the Fermi level and the conduction (valence) band for n- type (p-type) GaAs(001) surfaces and interfaces. These expressions are based on values for $E_{\rm CL} - E_{\rm VB}$ measured for clean n- and p-type GaAs(001)-(2×4) surfaces, which we have determined to be 18.81±0.04 eV and 18.85±0.04 eV for the n- and p-type surfaces, respectively. The resulting expressions are $\Delta E_{\rm CB\text{-}FL} = 20.23 - E_{\rm Ga3d}$ (eV) for n-type GaAs and $\Delta E_{\rm FL\text{-}VB} = E_{\rm Ga3d} - 18.85$ (eV) for p-type GaAs.

Finally, we have used angle-resolved XPS to determine the net surface and interface-state density n_s for both GaAs(001) free surfaces and Si/GaAs(001) heterojunctions. This quantity can be determined rather directly from core-level XPS measurements.[27] Solution of Poisson's equation for the GaAs depletion region yields a relation between the surface potential $\Phi(z=0)$ and n_s. Using n-type GaAs(001) from this investigation as an example, the surface potential is equal to $\Delta E_{\rm CB\text{-}EL}$ because the doping density (5×10^{17} cm^{-3}) is essentially equal to the effective density of conduction-band states for GaAs (4.7×10^{17} cm^{-3}). The value of $\Delta E_{\rm CB\text{-}FL}$ that is experimentally determined by XPS is actually an average value over the probing depth of the photoelectron, which is $\sim 3\lambda\sin\theta$. The attenuation length of Ga $3d$ photoelectrons excited with Al $K\alpha$ x rays propagating through GaAs is ~25 Å. Therefore, the probing depth for core-level measurements obtained at normal emission (~75 Å) constitutes a substantial fraction of the depletion width, which for the present n-type substrates is ~120 Å. In order to determine the true surface potential, we must integrate $\Phi(z)$ times an appropriate weighting factor to account for inelastic photoelectron attenuation over the depletion width, and equate this integral with $\Delta E_{\rm CB\text{-}FL}$. For computational purposes, it is convenient to integrate from the surface at $z=0$ to $z=\infty$. Doing so yields

$$\Delta E_{\rm CB\text{-}FL} = \Phi(\theta) = \frac{\int_0^\infty \Phi(z)\exp(-z/\lambda\sin\theta)dz}{\int_0^\infty \exp(-z/\lambda\sin\theta)dz} = \Phi(0)\left[1 - \left[\frac{2eN}{\varepsilon\Phi(0)}\right]^{1/2}(\lambda\sin\theta)\right] + \frac{eN\lambda^2\sin^2\theta}{\varepsilon} . \tag{2}$$

N is the bulk doping density and ε is the dielectric constant for GaAs. Equation (2) can be solved quadratically for $\Phi(0)$, which can then be used to determine n_s through solution of Poisson's equation according to the relation

$$n_s = \left[\frac{2\varepsilon N\Phi(0)}{e}\right]^{1/2} . \tag{3}$$

In Fig. 7 we show representative Ga $3d$ and Si $2p$ core-level spectra for clean surfaces of both n-type GaAs(001)-(2×4) and n-type Si(001)-(2×1), and heterojunctions composed of 9 Å (7 ML) of undoped Si and n^+-Si on n-type GaAs(001)-(2×4). The doping density

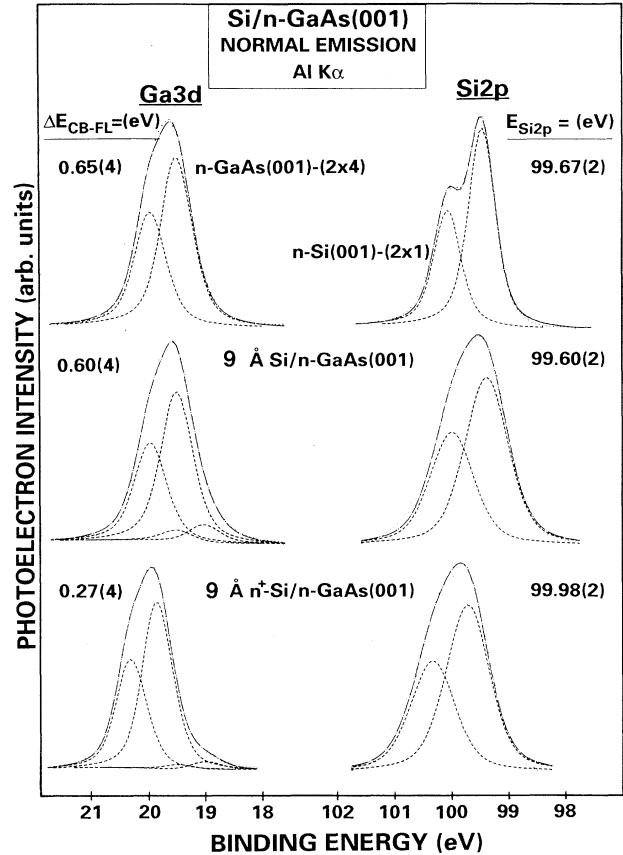

FIG. 7. Representative Ga $3d$ and Si $2p$ core-level photoemission spectra obtained at normal emission for undoped and As-doped Si overlayers on n-type GaAs(001), along with energy splittings between the conduction-band minimum and the Fermi level extracted from the Ga $3d$ spectra.

in the n-type Si(001) specimen was $\sim 1\times 10^{15}$ cm^{-3}. The branching ratio and spin-orbit splitting for all Ga $3d$ peaks were taken to be 0.65 and 0.46 eV, respectively. A mixed fitting function of 60% Gaussian and 40% Lorentzian character was used for each spin-orbit component. The branching ratio and spin-orbit splitting for the clean Si(001)-(2×1) surface Si $2p$ spectrum were fixed at 0.58 and 0.60 eV, respectively, while the fitting function was of 50% Gaussian and 50% Lorentzian character. However, the significant broadening of the Si $2p$ peak originating in the epitaxial layers (to be discussed below) made fitting these spectra very difficult. We attempted to decompose the Si $2p$ spectrum from a 3-ML film into three spin-orbit pairs corresponding to the slightly inequivalent bonding environments in each of the epitaxial layers. Each spin-orbit pair possessed the same peak parameters as those used to fit the clean Si(001)-(2×1) spectrum. While an excellent fit was obtained, the resulting intensities did not match what is expected on the basis of inelastic attenuation for photoelectrons emitted from three epitaxial layers and an abrupt interface. A certain amount of Si indiffusion occurs,[23] and this fact may provide a explanation for this discrepancy. Si indiffusion certainly does add further complications to the system. Furthermore, the lack of structure in the raw Si $2p$ spectra means that obtaining a unique fit is possible. Therefore, rather than attempt to carry out an elaborate multipeak fit, we have opted to fit all Si $2p$ spectra for the epitaxial layers with a single doublet, with a splitting of 0.60 eV and an intensity ratio that was allowed to vary from 0.58 to 0.68 in order to obtain the best fit. The centroid of this doublet then gives us a measure of the *average* binding energy over the inequivalent environments in the epifilm, which we denote as $E_{\mathrm{Si}\,2p}$.

Looking first at the Ga $3d$ spectra before and after Si overlayer growth, a second spin-orbit pair to lower binding energy from that of the substrate is required to obtain a good fit to the raw spectrum. We attribute these peaks to Ga-Si bonding at the interface. Our energy resolution is not sufficient to permit precise determination of the binding energy of the doublet. In fact, we found that the shift relative to the substrate doublet varied from -0.35 to -0.75 eV over the coverage range employed. Our primary goal was to determine the band bending as accurately as possible, and we found it necessary to let the binding-energy difference between the dominant substrate doublet and the much weaker reaction-product doublet vary over this range in order to obtain the best fit. The assignment of this doublet to Si-Ga bonding is consistent with the fact that the electronegativity of Si (1.7) is considerably less than that of As (2.2). Therefore, we expect the binding energy of Ga atoms bound to Si atoms to be less than for Ga atoms bound to As atoms, as is observed. The amount of Ga "consumed" in bonding to Si was, in general, found to be somewhat greater when Si was evaporated alone, as opposed to that associated with coevaporation with As. For instance, the numbers of Ga layers represented by the intensities in the reaction-product doublets in Fig. 8 are ~ 0.7 ML when Si is deposited alone and ~ 2 ML when Si and As are coevaporated. This result suggests that the absence of As_4 may result in

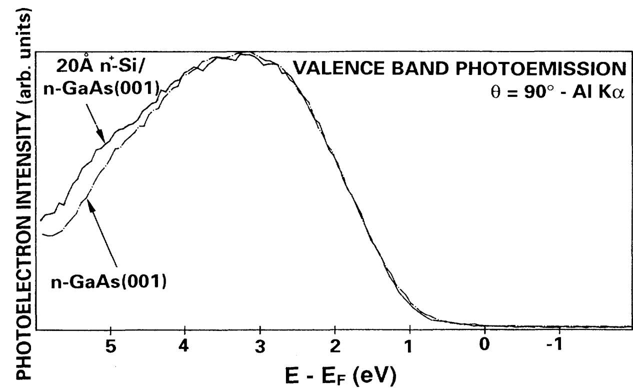

FIG. 8. Valence-band photoemission spectra obtained at normal emission for clean n-type GaAs(001) and a 20-Å deposit of As-doped Si on n-type GaAs(001). The negligible difference in the leading edge of the spectra near the Fermi level indicates that the full band discontinuity resides in the conduction band.

partial desorption of the surface As layer as the substrate equilibrates at the growth temperature 400 °C. Such desorption would expose more second-layer Ga atoms directly to Si atoms when the Si shutter is opened than would occur with the fully As-stabilized (2×4) surface.

The Si $2p$ binding energy for the undoped epilayer is quite close in value to that measured for lightly doped n-type Si(001)-(2×1), indicating that unintentionally doped Si on n-type GaAs(001) is actually nominally n type. This result probably arises because of the incorporation of trace amounts of As from the As-stabilized GaAs surface into the overlayer.

The Si $2p$ peak width in the epifilm spectrum (FWHM=1.30 eV) is considerably larger than that associated with the Si(100)-(2×1)(1.01 eV). In addition, a slight shoulder to high binding energy is seen. The high degree of structural order in the near-surface region of the Si(100)-(2×1) specimen implies that the vast majority of subsurface atoms are in identical structural environments. In addition, $\Delta E_{\mathrm{CB\text{-}FL}}$ in the bulk and at the surface of our Si(001)-(2×1) specimen were determined to be 0.26 and 0.35 eV, respectively, and the depletion width is ~ 1800 Å. Thus, band bending in negligible over the photoelectron probe depth (~ 75 Å), and this clean-surface spectrum provides an excellent reference in which the width is influenced only by the core-hole lifetime and the instrument resolution. In principle, the additional width seen in the Si $2p$ epilayer spectrum may be the result of slightly inequivalent electrostatic/bonding environments, strain, or band bending within the epilayer. The high binding-energy shoulder is most likely the result of interfacial bonding to As atoms, which possess an electronegativity of 2.2. The band bending is probably not extensive in the epilayer because the interface state density is sufficiently high that the pinned Fermi level at the free surface remains pinned after undoped Si is grown. We base this statement on the fact that band bending is the substrate remains substantial after epigrowth of undoped Si. One might expect that satisfaction of all interface bonds, as would occur for a perfect diamond/zinc-

blende interface, will eliminate gap states and flatten the bands. However, such is not the case. Using Eqs. (2) and (3), we estimate the net free-surface-state density to be $\sim 2.3\times 10^{12}$ cm^{-2}. There is a slight reduction in $\Delta E_{CB\text{-}FL}$ after growth of the undoped Si layer, but no substantial reduction in n_s. The Fermi level remains pinned near 0.6 eV below the conduction-band minimum, and the rather high density of interface charge probably terminates the space-charge region of the substrate, leaving the Si essentially field free. This conclusion is in agreement with that made by Silberman *et al.*, who measured substantial increases in the Ga $3d$ and $2p_{3/2}$ binding energies, but no change in the Si $2p$ binding energy in going from thin, epitaxial Si overlayers on p^+-GaAs(001) to the same on n^+-GaAs(001).[14] They interpreted this result in terms of a pinned Fermi level at the interface and a field-free Si overlayer. Therefore, we conclude that the additional width in the Si $2p$ epifilm spectrum is caused by some combination of strain and site inequivalency over the different layers in the film. This conclusion is supported by the fact that the Si $2p$ FWHM drops steadily from 1.30 eV at a coverage of 9 Å to 1.10 eV at an 80 Å coverage. Both strain and the influence of the interfacial layer are minimized at this thickness. In addition, the high binding-energy shoulder disappears with increasing coverage, which is consistent with the assignment of Si atoms bonded to As at the interface.

Looking again at the Ga $3d$ spectra, the GaAs bands flatten considerably when the Si overlayer is heavily doped with As compared to the situation when Si is undoped. In light of the fact that a Si $2p$ binding energy of 99.67 eV is indicative of a Fermi level ~ 0.35 eV below the conduction-band minimum for Si(001)-(2×1), the ~ 0.3-eV increase in the binding energy resulting from heavy As doping demonstrates that the doped epifilm is nearly degenerate n type. $\Delta E_{CB\text{-}FL}$ drops to 0.27 eV, indicating either a substantial reduction in interface-state density, or, more likely, a compensation of the positive space-charge region in the substrate by electrons from the overlayer.

These results occur consistently for a wide variety of coverages. A summary of the results are shown in Table I for deposits ranging from 9 to 80 Å. With the exception of the 80-Å coverage of unintentionally doped Si on p-type GaAs(001), there is only a slight reduction (increase) in band bending relative to the free surface for growth on n-type GaAs (p-type GaAs). These changes can be understood in terms of a partial compensation of the GaAs space-charge region by electrons from the unintentionally doped Si overlayer. However, there is no evidence that the Fermi level is unpinned in the sense that interface states are eliminated. In the event of Fermi-level unpinning by elimination of interface states, the bands would flatten substantially for both n- and p-type GaAs(001), as occurs when very high quality thin films of $Al_xGa_{1-x}As$ (Ref. 28) or $Ga_xAs_{1-x}Se$ (Refs. 29 and 30) are grown on GaAs. In this case, the interface-state density is considerably reduced, leading to little residual band bending. The 80-Å Si deposit on p-type GaAs may have resulted in a more extensive space-charge compensation due to the larger total number of carriers available by virtue of the greater film thickness. There is no change in behavior when we pass through the Si critical thickness. At this point, misfit dislocations are nucleated and presumably propagate to the interface. However, the Fermi level is already pinned, so there is no increase in band bending due to the introduction of additional defects.

Looking next to the data for the As-doped Si overlayers, we again see a substantial and consistent reduction

TABLE I. Absolute binding energies and derived electronic parameters from XPS analysis of Si/GaAs(001) heterojunctions.

Undoped Si deposit[a] (Å)	(ML-*EQ*)	$\Delta E_{CB\text{-}FL}$	On n-type GaAs $E_{Si\,2p}$	ΔE_{CL}	ΔE_{VB}[b]	$\Delta E_{CB\text{-}FL}$	On p-type GaAs $E_{Si\,2p}$	ΔE_{CL}	ΔE_{VB}[b]
0	(0)	0.65				0.44			
9	(7)	0.60	99.60	79.97	0.56	0.52	99.50	80.13	0.40
20	(15)	0.61	99.53	79.91	0.62	0.57	99.49	80.07	0.46
40	(30)	0.56	99.57	79.90	0.63	0.54	99.55	80.16	0.37
80	(60)	0.57	99.55	79.89	0.64	0.65	99.52	80.02	0.51
As doped Si deposit[a] (Å)	**(ML-*EQ*)**	**$\Delta E_{CB\text{-}FL}$**	**On n-type GaAs $E_{Si\,2p}$**	**ΔE_{CL}**	**ΔE_{VB}[b]**	**$\Delta E_{FL\text{-}VB}$**	**On p-type GaAs $E_{Si\,2p}$**	**ΔE_{CL}**	**ΔE_{VB}[b]**
0	(0)	0.65				0.44			
9	(7)	0.27	99.95	79.99	0.54				
20	(15)	0.29	99.92	79.98	0.55	0.77	99.81	80.19	0.34
40	(30)	0.36	99.87	80.00	0.53	0.87	99.96	80.24	0.29
80	(60)	0.39	99.99	80.15	0.38	0.84	100.08	80.39	0.14

[a]Deposit thickness determined by RSB-calibrated quartz thickness oscillator. The uncertainties in $\Delta E_{CB\text{-}FL}$, $E_{Si\,2p}$, and ΔE_{CL} are ±0.04, ±0.02, and ±0.03 eV, respectively.
[b]ΔE_{VB} values in this column were determined by the core-level method described in the text. The uncertainty in ΔE_{VB} is ±0.07 eV.

(increase) in band bending for growth on n-type GaAs (p-type GaAs). In all cases, the Si is degenerately or nearly degenerately doped n type. These large changes in band bending can be understood in terms of a significant reduction (increase) in the electric field across the depletion region brought about by electron charge transfer from the Si overlayer to the substrate, rather than by the elimination of interface states. Electron transfer from the overlayer into the bulk is expected for both n- and p-type substrates as the Fermi levels equilibrate upon formation of the heterojunction. Such charge transfer will reduce the net electric field across the depletion region of n-type GaAs and will increase the field for p-type GaAs. The net positive charge in the thin Si overlayer will effectively reduce (enhance) the interface charge density of n-type GaAs (p-type GaAs). Using Eqs. (2) and (3), we can estimate the change in the interface charge density brought about by this charge transfer. These equations predict a drop from $\sim 2.3\times10^{12}$ cm^{-2} to $\sim 1.5\times10^{12}$ cm^{-2} for n-type GaAs, and an increase from $\sim 1.9\times10^{12}$ cm^{-2} to $\sim 2.5\times10^{12}$ cm^{-2} for p-type GaAs. This result is consistent with modeling results by Sambell and Wood, in which they predict compensation of interface-state charge when the interface state density is 10^{13} cm^{-2} and the n-type Si doping exceeds 2×10^{18} cm^{-3}.[15]

It is of interest to inquire about the role of As concentration on the starting surface in affecting band bending at the Si/GaAs interface. It might be argued that the band bending is influenced by the presence or absence of excess As on the starting surface, in addition to the dopant level in the Si overlayer. However, recent high-resolution core-level studies of GaAs(001) surfaces with the full range of surface As concentration show negligible changes in band bending with surface composition.[31] Therefore, the changes in band bending we observe are clearly the result of doping in the Si layer.

We next consider the question of determining the band offset. As discussed above, the effect that strain has on the valence-band offset is difficult to precisely determine when using core-level binding energies. This problem occurs primarily because of the need to accurately measure the core-level to valence-band-maximum energy difference for the strained semiconductor. In the present case, the problem is further complicated by the breadth of the Si $2p$ spectra from the epifilms, the origin of which is discussed above. We include in Table I values of $\Delta E_{\rm VB}$ calculated from core-level binding energies using the extrapolated values of δ_s for full strained Si on GaAs from Yu *et al.*[26] A rather wide spectrum of values is predicted, ranging from 0.14 eV for 80 Å of As-doped Si on p-type GaAs to 0.64 eV for 80 Å of unintentionally doped Si on n-type GaAs. These discrepancies indicate that the core-level method cannot be used reliably for such systems. As an alternative, we have measured the valence-band spectrum directly for 20 Å of n^+-doped Si on n-type GaAs(001), and have compared with the analogous spectrum for the clean surface. The core-level analysis predicts a value of 0.55 eV for $\Delta E_{\rm VB}$. In Fig. 8, we show the valence-band spectrum for this heterojunction, obtained at normal emission, overlapped with that from a clean n-type GaAs(001) surface. We have shifted the clean-surface spectrum to higher binding energy to correct for the differences in band bending between the two surfaces, and to allow for maximum overlap. Clearly, there is no significant difference in the leading edge of the two valence bands. The attenuation length for Al $K\alpha$-excited valence-band electrons is ~ 25 Å in both Si and GaAs. Therefore, the total probe depth at normal emission is ~ 75 Å, and both the substrate and overlayer valence bands should contribute to the total spectrum in a measurable way. A valence-band offset of $\sim\geq 0.1$ eV should be readily visible in the spectrum for the heterojunction. However, the extremely high degree of similarity between the clean-surface and heterojunction spectra indicates that $\Delta E_{\rm VB}$ is ~ 0 eV. Thus, the entire band offset (~ 0.3 eV) is in the conduction band, in agreement with current-voltage measurements of Al/Si/GaAs(001) samples.[32]

IV. CONCLUSIONS

We have examined the chemical, structural, and electronic properties of Si overlayers on n-type and p-type GaAs(001)-(2×4). Our goal was to investigate the influence of such Si overlayers on band bending in the depletion region of GaAs(001), and to see how the electronic properties of the interfacial region depend on structure and interface chemistry. We find that limited interfacial reaction between Si and Ga occurs for all coverages studied. The critical thickness was determined to be 10 ± 1 Å, and the lattice constants parallel and perpendicular to the interface were measured to be 5.65 Å and 5.32 ± 0.10 Å, respectively. Undoped Si overlayers preserve the band bending found on clean surfaces of both n- and p-type GaAs(001) for coverages below and above the critical thickness, while heavily As-doped Si layers substantially flatten the bands on n-type GaAs, while increasing band bending on p-type GaAs. Thus, it appears that epitaxial growth of Si does not unpin the Fermi level in the sense of eliminating interface states. Rather, heavy n-type doping in the Si overlayer reduces (increases) band bending on n-type (p-type) GaAs by inducing electron transfer into the depletion region and effectively lowering (increasing) the electric field across the space-charge region.

ACKNOWLEDGMENTS

The authors would like to thank B. E. Weir and L. C. Feldman for performing the RBS calibration of our coverage scale, and R. T. Jobe for carrying out the AFM measurements.

*Present address: Molecular Science Research Center, Pacific Northwest Laboratory, P.O. Box 999, MS K2-12, Richland, WA 99352.

[1] S. M. Sze, *Physics of Semiconductor Devices,* 2nd ed. (Wiley-Interscience, New York, 1981), Chap. 5.

[2] A. Piotrowska, A. Guivarch and G. Pelous, Solid-State Electron. **26**, 179 (1983), and references therein.

[3] R. W. Grant and J. R. Waldrop, J. Vac. Sci. Technol. B **5**, 1015

(1987).
[4]J. R. Waldrop and R. W. Grant, Appl. Phys. Lett. **52**, 1794 (1988).
[5]J. R. Waldrop and R. W. Grant, J. Vac. Sci. Technol. B **6**, 1732 (1988).
[6]S. A. Chambers and T. J. Irwin, Phys. Rev. **38**, 7484 (1988).
[7]S. A. Chambers and T. J. Irwin, Phys. Rev. **38**, 7858 (1988).
[8]G. Bratina, L. Sorba, A. Antonini, G. Baisiol, and A. Franciosi, Phys. Rev. B **45**, 4528 (1992).
[9]S. Tiwari, S. L. Wright, and J. Batey, IEEE Electron. Dev. Lett. **ED-9**, 488 (1988).
[10]G. G. Fountain, S. V. Hattangady, D. J. Vitkavage, R. A. Rudder, and R. J. Markunas, Electron. Lett. **24**, 1134 (1988).
[11]H. Hasegawa, M. Akazawa, K. Matsuzaki, H. Ishii, and H. Ohno, Jpn. J. Appl. Phys. **27**, L2265 (1988).
[12]J. L. Freeouf, J. A. Silberman, S. L. Wright, S. Tiwari, and J. Batey, J. Vac. Sci. Technol. B **7**, 854 (1989).
[13]J. L. Freeouf, D. A. Buchanan, S. L. Wright, T. N. Jackson, and B. Robinson, Appl. Phys. Lett. **57**, 1919 (1990).
[14]J. A. Silberman, T. J. De Lyon, and J. M. Woodall, Appl. Phys. Lett. **59**, 3300 (1991).
[15]A. J. Sambell and J. Wood, IEEE Trans. Electron. Dev. **TED-37**, 88, (1990).
[16]J. Massies, P. Etienne, F. Dezaly, and N. T. Linh, Surf. Sci. **99**, 121 (1980).
[17]S. A. Chambers, Adv. Phys. **40**, 357 (1991).
[18]G. Bratina, L. Sorba, A. Antonini, L. Vanzetti, and A. Francoisi, J. Vac. Sci. Technol. B **9**, 2225 (1991).
[19]S. A. Chambers and V. A. Loebs, Phys. Rev. B **42**, 5109 (1990).
[20]S. Tanuma, C. J. Powell, and D. R. Penn, Surf. Int. Anal. **11**, 577 (1988).
[21]R. Z. Bachrach, R. D. Bringans, M. A. Olmstead, and R. I. G. Uhrberg, J. Vac. Sci. Technol. B **5**, 1135 (1987).
[22]P. C. Zalm, P. M. J. Maree, and R. I. J. Olthof, Appl. Phys. Lett. **46**, 597 (1985).
[23]Detailed XPD studies of the 1-ML Si/GaAs(001) interface reveal that a substantial fraction of the Si monolayer indiffuses, occupying both cation and anion lattice sites down to the third atomic layer (the first layer being the surface layer).
[24]J. Tersoff and C. G. Van de Walle, Phys. Rev. Lett. **59**, 946 (1987).
[25]G. P. Schwartz, M. S. Hybertsen, J. Bevk, R. G. Nuzzo, J. P. Mannaerts, and G. J. Gualtieri, Phys. Rev. B **39**, 1235 (1989).
[26]E. T. Yu, E. T. Croke, T. C. McGill, and R. H. Miles, Appl. Phys. Lett. **56**, 569 (1990).
[27]T. Ogama, J. Appl. Phys. **64**, 6469 (1988).
[28]S. A. Chambers, V. A. Loebs, and D. H. Doyle, J. Vac. Sci. Technol. B **8**, 985 (1990).
[29]S. A. Chambers and V. S. Sundaram, Appl. Phys. Lett. **57**, 2342 (1990).
[30]S. A. Chambers and V. S. Sundaram, J. Vac. Sci. Technol. B **9**, 2256 (1991).
[31]G. LeLay, D. Mao, A. Kahn, Y. Hwu, and G. Margaritondo, Phys. Rev. B **43**, 14301 (1991).
[32]J. C. Costa, F. Williamson, T. J. Miller, K. Beyzavi, M. I. Nathan, D. S. L. Mui, S. Strite, and H. Morkoç, Appl. Phys. Lett. **58**, 382 (1991).

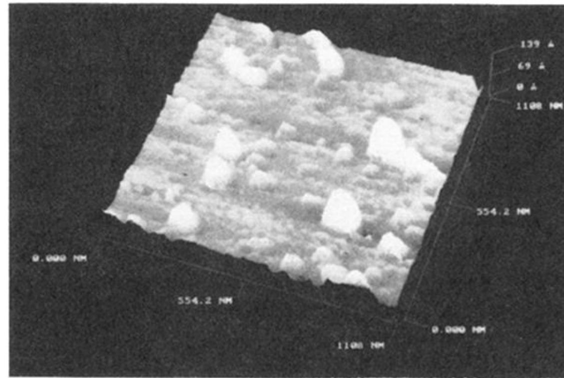

FIG. 2. AFM image of a 60-Å Si deposit, as judged by the QCO. The film thickness based on Ga 3*d* attenuation was 34 Å. The tendency of Si to form islands on GaAs is the result of its higher surface-free energy. The presence of islands explains the discrepancy between the QCO film thickness and the thickness based on Ga 3*d* attenuation.

5Å (3 ML) (2x1)-Si/n-GaAs(OO1)

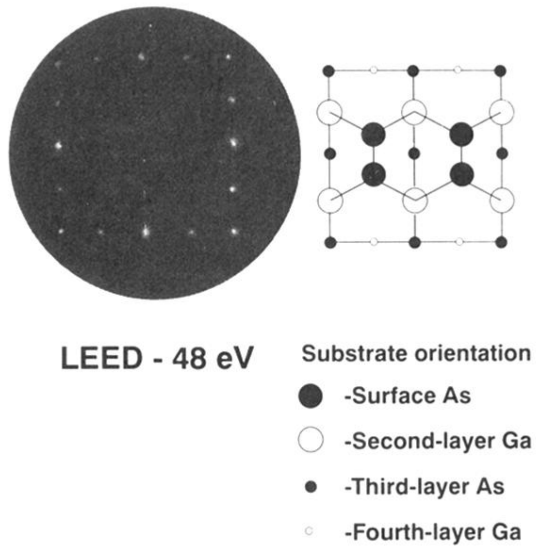

FIG. 3. Orthogonal (2×1) (LEED) patterns for a 5-Å epitaxial overlayer of Si on GaAs(001), grown at 400 °C. At the right is a structural diagram of the substrate showing the substrate crystal orientation relative to the overlayer LEED pattern.